Polymer 49 (2008) 2235–2242

Contents lists available at ScienceDirect

Polymer

journal homepage: www.elsevier.com/locate/polymer

Influence of initiators on the growth of poly(ethyl 2-cyanoacrylate) nanofibers

Pratik J. Mankidy [a], Ramakrishnan Rajagopalan [b], Henry C. Foley [a,b,c,*]

[a] Department of Chemical Engineering, The Pennsylvania State University, University Park, PA 16802, United States
[b] Materials Research Institute, The Pennsylvania State University, University Park, PA 16802, United States
[c] Department of Chemistry, The Pennsylvania State University, University Park, PA 16802, United States

ARTICLE INFO

Article history:
Received 19 October 2007
Received in revised form 4 March 2008
Accepted 5 March 2008
Available online 14 March 2008

Keywords:
Polymer nanofibers
Poly(ethyl 2-cyanoacrylate)
Synthesis

ABSTRACT

The type of anionic initiator used to polymerize ethyl 2-cyanoacrylate was found to influence the morphology of the polymer formed via vapor phase polymerization. Depending upon the type of initiator, polymerization of ethyl 2-cyanoacrylate resulted in either the formation of neat polymer nanofibers (~200 nm in diameter) or thin films. Based on the classification of anions using Hard Soft Acid Base principles, we found that *harder* anions favored polymer film formation while *softer* ones favored polymer nanofibers. Infrared (IR) spectroscopy, scanning electron microscopy (SEM) and gel permeation chromatography (GPC) were used to characterize the structure, morphology and molecular weight of the synthesized polymers, respectively. Finally, a mechanism of formation of different polymer morphologies is proposed.

1. Introduction

The importance of polymer nanofibers is apparent from the vast volume of literature in recent years focusing on synthesis methods, properties and applications of nanofibers. Nanofibrous polymer structures offer a high surface area to volume ratio which can be exploited for a variety of applications as summarized by recent reviews [1,2]. These applications include making use of the mechanical properties of nanofibers for reinforced composites [3], tissue scaffolding material [4], controlled drug delivery applications [5] or as filtration media [6].

Currently there are two major approaches for the fabrication of polymer nanofibers, template-based methods or electrospinning. Template-based methods [7] involve either extrusion of a polymer melt through nano-sized pores of a template, for example through an anodized aluminum oxide membrane [8] or extrusion polymerization of polymer nanofibers via catalyst immobilized on the walls of a nanotemplate, such as mesoporous silica [9]. This method, however, makes removal of the fibers from the template complex. Electrospinning [1,2] involves the use of a high voltage source to generate electrically charged polymer jets, which are collected on a substrate as a mat of nanofibers. This technique necessitates that the polymer be either melt or solvent processable and be able to withstand the high voltage electric fields. A lesser used approach for polymer nanofibers formation is template-less formation of nanofibers during polymerization. Polyaniline nanofibers have been synthesized this way either extrinsically by adding 'structure-directing' agents during polymerization [10], or intrinsically by interfacial polymerization schemes [11]. Polyacetylene fibrils ranging in diameters from 3–20 nm have also been reported for certain conditions of Ziegler–Natta polymerized acetylene [12]. This synthesis method of polymer nanofibers presents an interesting and truly 'bottom-up' route that is an alternative to template-based processes or electrospinning for the mass production of nanofibers.

We recently demonstrated a novel technique for facile growth of poly(ethyl 2-cyanoacrylate) [PECA] nanofibers without a template by vapor phase polymerization of the ethyl 2-cyanoacrylate [ECA] monomer [13]. ECA commonly known as Superglue® undergoes anionic polymerization initiated by a variety of covalent or ionic bases, including water [14]. Scheme 1 illustrates this polymerization via initiation by a nucleophile (Nu^-) and propagation by subsequent addition of ECA monomer units to the carbanion end of the growing chain.

In our previous studies, it was observed that vapor phase polymerization of ECA carried out under high relative humidity conditions resulted in different morphologies of the polymer depending upon the type of initiator used. For certain initiators, such as NaCl, a mass of nanofibers were obtained, while for other initiators, for example NaOH, a textured polymer film was obtained. In a relevant study, Doiphode et al. [15] grew similar nanofibers of polycyanoacrylate on electrospun fibers by first exposing the electrospun fibers to water vapor and then to cyanoacrylate vapor. The water vapor condenses as tiny droplets on the electrospun fibers thereby rendering tiny islands of initiator that start the

* Corresponding author. Department of Chemical Engineering, The Pennsylvania State University, University Park, PA 16802, United States.
E-mail address: hfoley@ist.psu.edu (H.C. Foley).

0032-3861/$ – see front matter © 2008 Elsevier Ltd. All rights reserved.
doi:10.1016/j.polymer.2008.03.018

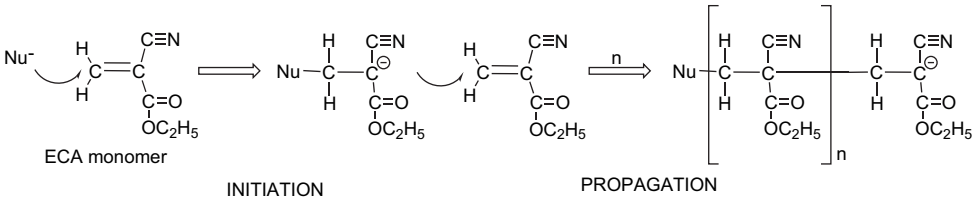

Scheme 1. Initiation by nucleophile (Nu^-) and propagation steps for ethyl 2-cyanoacrylate polymerization.

polymerization reaction. The authors propose an explanation for nanofiber formation by drawing an analogy to vapor–liquid–solid mechanism for whisker growth [16,17]. However, our observation has shown that we can obtain different polymer morphologies under the same conditions of high relative humidity using different initiators. In this paper, we report the study of polymerization of ECA vapor on substrates coated with initiators resulting in either polymer films or fibers. A classification of these initiators is proposed that explains the basis of polymer film versus fiber formation. The polymer nanofibers and films were characterized by infrared (IR) spectroscopy, scanning electron microscopy (SEM) and molecular weight of the polymer was measured by gel permeation chromatography (GPC). The mechanism of formation of the different morphologies is discussed based on the results.

2. Experimental methods

2.1. Materials

ECA monomer was used as received (>95% purity, Sirchie Fingerprint Laboratories Inc.). The initiator compounds, NaI, NaBr, NaCl, NaH_2PO4, Na_2SO_4, CH_3COONa, Na_2HPO_4, NaOH, Na_3PO_4, Na_2CO_3 and $NaHCO_3$, were all ACS reagent grade and used as received (Sigma–Aldrich). Water used in this study was Nanopure water obtained from a Barnstead™ purification system.

2.2. Polymerization

Vapor phase polymerization of ECA was carried out in an enclosed chamber. Relative humidity inside the chamber was maintained at ~95% at room temperature using an 8% by wt. aqueous sulfuric acid solution in the chamber for all fuming experiments. Each initiator compound was spin coated onto a clean Si wafer from a 0.2 M aqueous solution of the salt. Approximately 1 ml of solution was deposited onto the wafer by spin coating at a speed of ~1600 rpm. The wafer was dried and placed in the chamber at 95% RH for a period of 10 h, after which ~2 g of liquid ECA monomer was introduced into a separate container inside the chamber. After sufficient time for polymerization (12 h), the wafers coated with polymer residue, were removed and characterized.

2.3. Characterization

Scanning electron microscopy was done using a JEOL 6700F Field Emission SEM. Samples were first sputtered with a thin film of gold to minimize charging effects by the electron beam. Infrared spectroscopy was done using attenuated total reflectance IR (ATR-IR) on representative samples of polymer taken from the surface of the Si wafer on which they were prepared. A Bruker IFS 66/S instrument acquiring data in the mid-IR (4000–400 cm^{-1}) range was used to collect the spectra. Molecular weight estimation of the polymer samples was done using GPC (Waters HPLC fitted with a StyragelHR column) with tetrahydofuran (THF) as the solvent and a polystyrene calibration standard.

3. Results and discussion

Vapor phase polymerization of ECA under the same high relative humidity conditions using different initiators resulted in a polymer either in the form of nanofibers as shown in Fig. 1(a) or as a continuous, textured film depicted in Fig. 1(b). The nanofibers were obtained, when 0.2 M Na_2HPO_4 is the initiator and the film morphology was obtained using 0.2 M Na_3PO_4 as the initiator. The size of the fibers ranged between 150 and 250 nm. The two kinds of morphologies signifying 1-D (fiber) and 2-D (film) growth of the polymer clearly showed the influence of the type of initiators. As this polymerization occurs via an anionic mechanism, we studied the characteristics of the anionic initiator and its effect on the polymer morphology in detail.

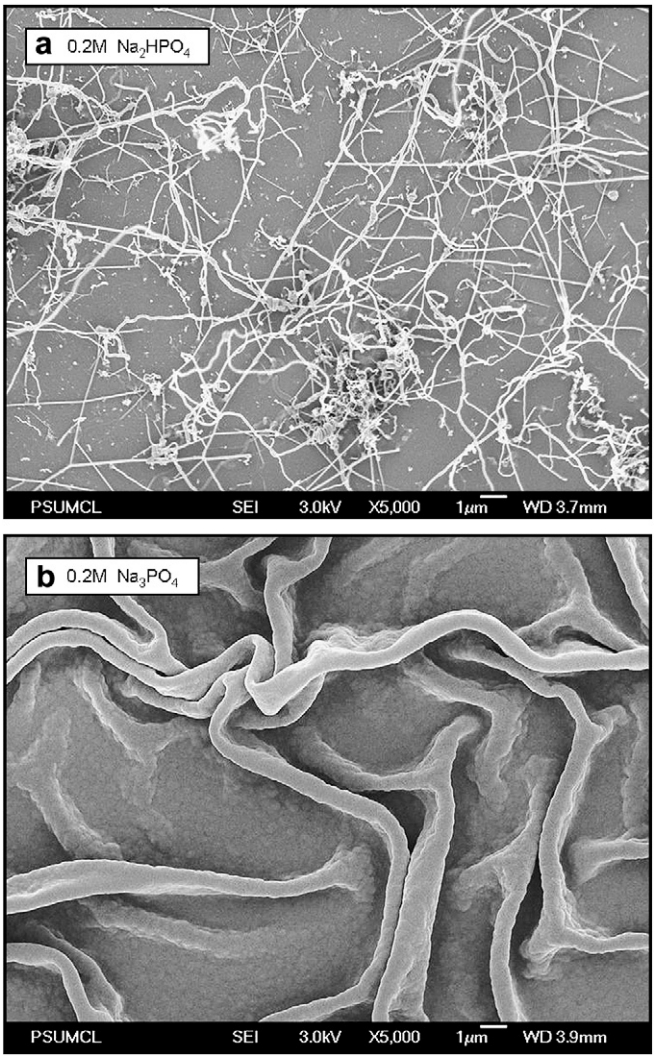

Fig. 1. SEM images of PECA morphology obtained from vapor phase polymerization on substrates spin coated with (a) 0.2 M Na_2HPO_4 and (b) 0.2 M Na_3PO_4. Scale bars are 1 μm.

3.1. Classification of initiators

Several initiators were examined for the type of polymer morphology that they developed. Fig. 2 shows SEM images of the polymer grown using a few of those different initiators. The cation (Na) for the different anionic initiators was kept the same for consistency. It was observed that the chloride, monophosphate, diphosphate and sulfate anions resulted in the formation of polymer nanofibers while the acetate, hydroxide, triphosphate, carbonate and bicarbonate anions resulted in the formation of the polymer film. Interestingly, iodide and bromide anions were unable to initiate polymerization of the monomer from the vapor phase and resulted in no polymer being deposited at all under the same conditions. The nanofibers obtained were similar to those observed by us [13] and others [15]. The diameters of the fibers were roughly in the range of 150–200 nm. The polymer film obtained was continuous but also appears convoluted. A noteworthy observation was that for the initiators examined, a given initiator only resulted in one kind of polymer morphology, i.e. from an initiator that resulted in polymer nanofibers, no polymer film was observed and vice versa.

Also, the concentration of the spin-coated solution did not seem to affect the polymer morphology. Polymer grown on Si wafers spin coated with 0.2 M and 1 M NaOH solutions resulted in identical polymer films and polymer grown on wafers spin coated with 0.2 M and 1 M NaCl solutions gave identical polymer nanofibers. This phenomenon, that a particular anion always initiated polymerization to develop the same exclusive morphology (film or fiber), suggests an inherent growth directing or 'templating' effect occurring during the initiation step which was influenced by the type of anionic initiators used for ECA polymerization.

To observe the effect of a different cation, as an example, 0.2 M solutions of KOH and KCl were also spin coated on substrates and examined for the type of polymer morphology they developed. Fig. 3(a) and (b) shows SEM images of polymer grown on these substrates. The morphologies observed, i.e. film for hydroxide ion and fibers for chloride ion, are in agreement with those observed for initiation using NaOH and NaCl, thereby suggesting that the morphology of the polymer obtained was inherently dependent only on the type of anion used for initiation.

The morphology of the spin-coated material (initiator) was also observed prior to polymerization in order to examine the influence, if any, of the morphology of the underlying initiator layer on the morphology of the resultant polymeric material. Again as an example, 0.2 M solutions of NaOH and NaCl were spin coated onto Si substrates, dried and viewed using SEM (Fig. 4). The SEM images confirm that the underlying spin-coated initiator does not resemble the morphology of the polymer (film or fiber) grown on these substrates. Thus polymer morphology must be a function of the polymerization mechanism itself.

We have previously observed [13] that the presence of a high relative humidity (95% RH) atmosphere during the polymerization process was essential for neat polymer nanofiber formation. The high relative humidity is required for solvating the ions of the spin-coated initiator, but water is also known to be an effective initiator itself for the polymerization of ECA [14,15]. Hence it was important to examine the hygroscopicity of the initiator compounds studied as the amount of water taken up by different initiators. Table 1 shows the amount of water taken up by each initiator after being placed in a 95% RH environment for a period of 20 h on the basis of grams of water uptake per gram of dry solid. The table lists the initiators in the order of increasing water uptake and also depicts the corresponding polymer morphology observed by SEM. There appears to be no correlation between the hygroscopicity of the initiator and the polymer morphology.

For example, Na_2SO_4 which had an uptake of 1.61 g of water/g of dry solid and NaCl which had a water uptake of 5.23 g of water/g of dry solid, both resulted in polymer nanofibers being formed. But by contrast Na_3PO_4 and NaOH that had uptakes of 2.16 and 5.67 g of water/g of dry solid, respectively, resulted in polymer films. Also NaI and NaBr that had water uptake amounts similar to those of KCl and CH_3COONa, respectively, caused no polymerization at all.

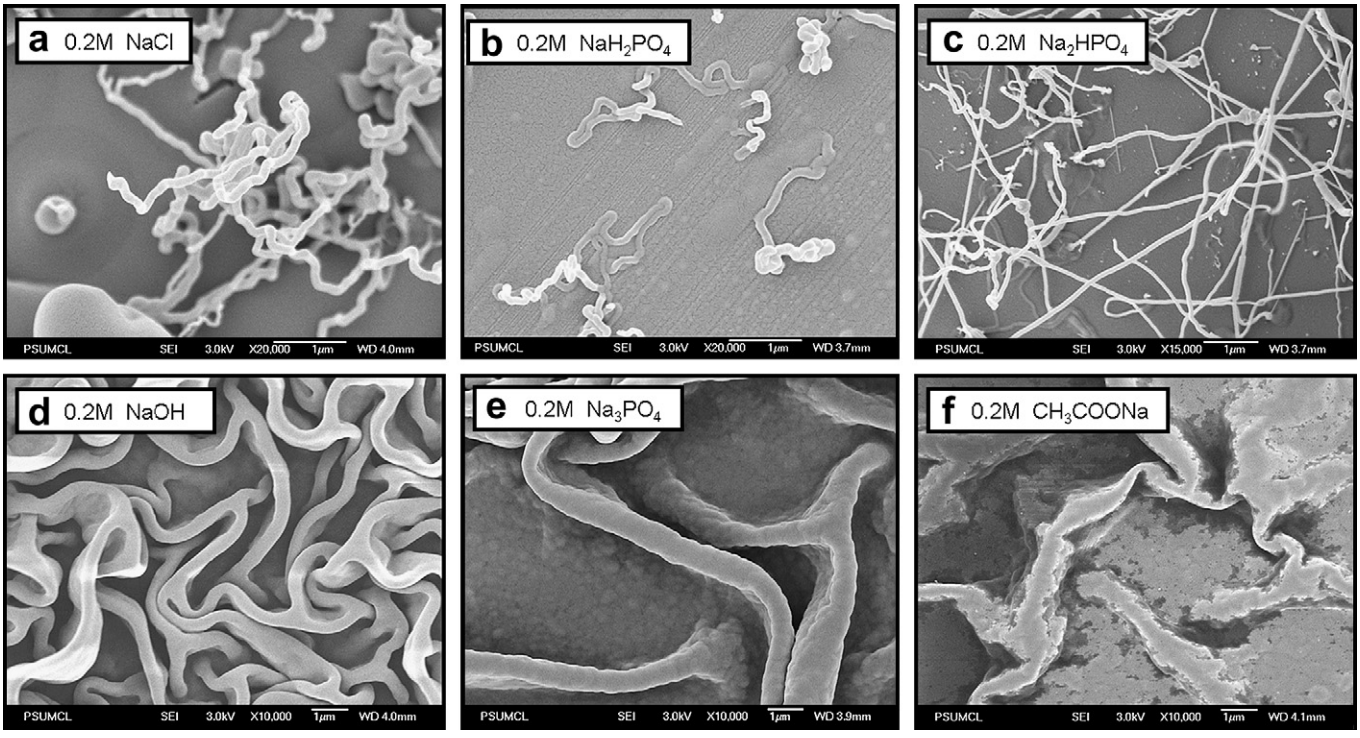

Fig. 2. SEM images of different polymer morphologies obtained by vapor phase polymerization on substrates spin coated with different anionic initiators at the same concentration of 0.2 M. All scale bars are 1 μm.

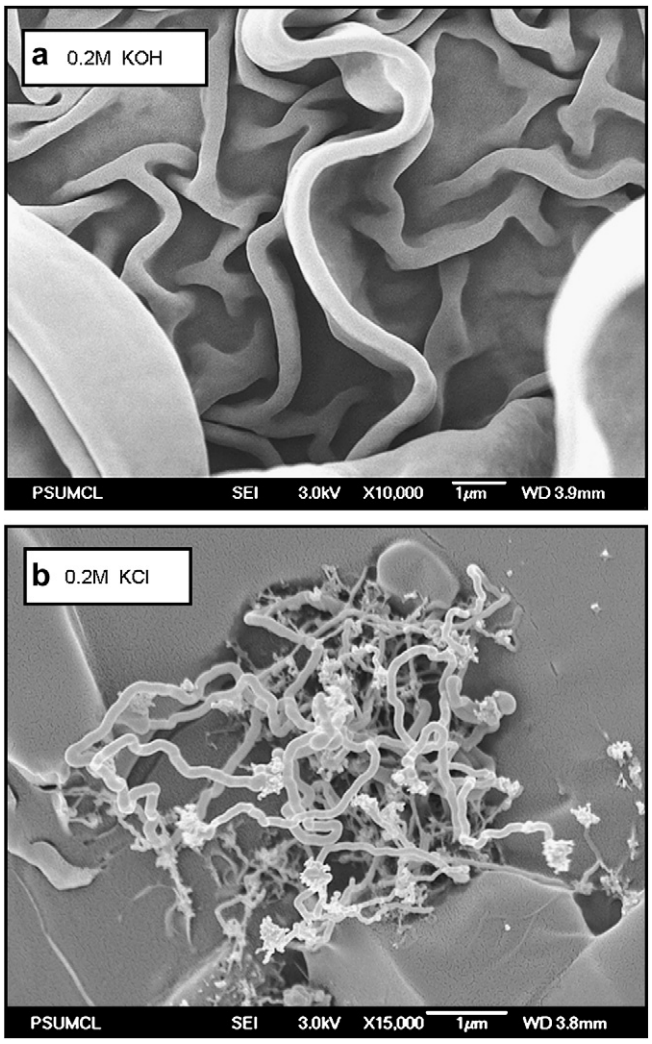

Fig. 3. SEM images of polymer morphologies observed for polymerization using (a) 0.2 M KOH and (b) 0.2 M KCl as initiators. Scale bars shown are 1 μm.

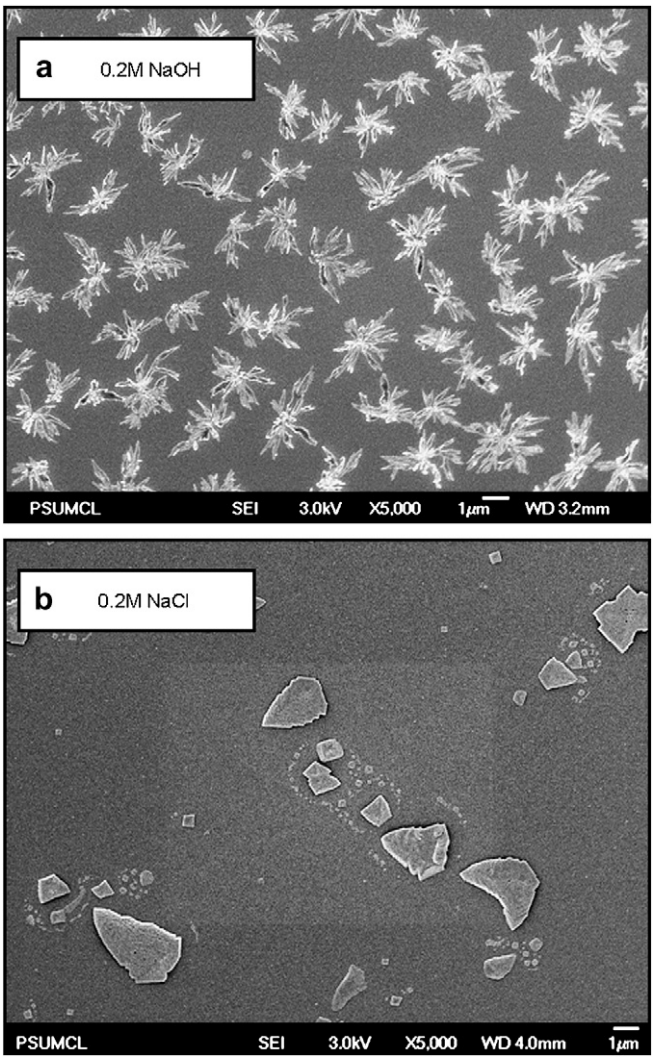

Fig. 4. SEM images of spin coated (a) 0.2 M NaOH and (b) 0.2 M NaCl solutions after drying on Si substrates prior to polymerization.

A classification of the initiators on the basis of the relative softness–hardness of the anions proved to be a more viable explanation for the different morphologies observed. The Hard Soft Acid Base (HSAB) theory developed by Pearson [18,19] defines hard acids or bases as small, slightly polarizable species and soft acids and bases as larger, easily polarizable species. The HSAB principle suggests the following general rule of thumb for qualitatively estimating the stability of acid–base complexes *hard acids prefer to associate with hard bases and soft acids prefer to associate with soft bases*. This statement implies that acids or bases can be classified as hard or soft by a measure of their apparent preference to react with other hard or soft species. In order to classify the anionic initiators in this investigation a comparison was made between the preference of an anionic species $[B^-]$ to bind with a soft acid, methylmercury cation CH_3Hg^+ (pK_s values) and its preference towards the hard acid H^+ (pK_a values). Here $pK_a = \log[HB]/[H^+][B^-]$ and $pK_s = \log[CH_3HgB]/[CH_3Hg^+][B^-]$. Large pK_s values then imply a strong affinity for the soft acid and, therefore, are an indication of $[B^-]$ possessing a *soft* character. Similarly, higher pK_a values represent a greater affinity for the hard acid, and thus reflect a *hard* character for $[B^-]$. To obtain a measure of the relative soft–hard character of the anions it is necessary to consider both pK_s and pK_a, hence we looked at the difference between the pK_s and pK_a values. Larger $pK_s - pK_a$ values indicated a *softer* anion and smaller $pK_s - pK_a$ values represent a *harder* anion. Table 2 lists the anionic initiators along their respective pK_s and pK_a values and the corresponding morphology of the polymer observed by SEM. The pK_s and pK_a values shown in Table 2 were obtained from reports published in the literature [20–24]. For certain anions whose pK_s values were unavailable, estimations were made for their values. The list in Table 2 is arranged from the top in decreasing order of $pK_s - pK_a$ values. Interestingly, the corresponding observed polymer morphology follows a trend with the decreasing $pK_s - pK_a$ values. For

Table 1
Water uptake of different initiators for ECA polymerization and the morphology observed by SEM

Initiator	Water uptake (g of water /g dry solid)	Polymer morphology
$NaHCO_3$	Not measurable	Film
Na_2SO_4	1.61	Fiber
Na_3PO_4	2.16	Film
NaH_2PO_4	2.95	Fiber
Na_2HPO_4	3.07	Fiber
KCl	3.23	Fiber
NaI	3.37	No polymer
Na_2CO_3	3.66	Film
NaBr	4.37	No polymer
CH_3COONa	4.94	Film
NaCl	5.23	Fiber
KOH	5.67	Film
NaOH	7.70	Film

Table 2
Classification of initiators on the basis of their relative softness/hardness

Anion	pK_s	pK_a	$pK_s - pK_a$	Morphology
I^-	8.6[a]	−9.5[a]	18.1	No polymer
Br^-	6.62[a]	−9[a]	15.62	No polymer
Cl^-	5.25[a]	−7[a]	12.25	Fiber
$H_2PO_4^-$	>5.03*	2.12[e]	>2.91	Fiber
SO_4^{2-}	2.64[d]	1.92[e]	0.72	Fiber
CH_3COO^-	3.36[b]	4.54[b]	−1.18	Film
HPO_4^{2-}	5.03[a]	6.79[a]	−1.76	Fiber
OH^-	9.37[a]	15.7[a]	−6.33	Film
PO_4^{3-}	<5.03*	12.67[e]	<−7.64	Film
CO_3^{2-}	1.89[c]	10.25[e]	−8.36	Film
HCO_3^-	>1.89*	6.37[e]	>−4.48	Film

*Qualitative estimates based on relative size and polarizability.
[a] Ref.[20].
[b] Ref. [21].
[c] Ref. [22].
[d] Ref. [23].
[e] Ref. [24].

the larger values of $pK_s - pK_a$, (greater than 12.25) i.e. the softest anions investigated, no polymer formation was observed. For an intermediate range of $pK_s - pK_a$ values from 12.25 to −1.76, the anions appear to possess a certain soft–hard character that is favored for polymer nanofiber formation. For values below that range i.e. the harder anions, only the textured film-like polymer morphology was observed. The only exception from the general trend was the acetate ion which had resulted in a polymer film, but had a $pK_s - pK_a$ value of −1.18. This could be attributed to variations of the pK_s and pK_a values obtained from the literature. This classification then implies that it is possible to distinguish between nanofiber-yielding initiators and polymer film-yielding initiators based on their relative soft–hard character.

The HSAB principle has been widely and successfully applied to explain experimental observations in organic chemistry [25–27]. Qualitative correlations have been made based on the hard–hard, soft–soft interaction principles to rationalize the thermodynamic stability of acid–base complexes and the kinetics of their formation. The general rule with respect to kinetics states that *hard electrophiles react quickly with hard nucleophiles and soft electrophiles react quickly with soft nucleophiles*. With regard to ECA polymerization, initiation is the interaction between an electrophile and a nucleophile. Because of the strong electron withdrawing effect of the –CN and $–COOC_2H_5$ groups, the double bond in the monomer is slightly polarized rendering the β-carbon atom susceptible for nucleophilic attack by the anionic species [14]. This slightly positive center then acts as a hard acid center because of its positive charge and low polarizability. The trend observed in Table 2 implies that as the soft character $pK_s - pK_a$ of the initiating anion decreases, or conversely as the hard character increases, the rate of initiation becomes faster because of an increased hard–hard nature of the interaction between the anion and the monomer which results in polymer film formation. Whereas, when the interaction is between a softer anionic initiator and the hard center of the monomer, the rate of initiation is relatively slower and the resulting polymer morphology obtained is nanofibrous. Table 2 also then indicates that for initiators that are even softer, no initiation takes place at all for the vapor phase monomer as no polymer is deposited for those initiators (iodide and bromide ions). However, it must be pointed out that in the liquid phase these initiators are capable of initiating polymerization [28].

Hence the classification of the initiators in terms of their relative soft–hard character in fact points to a distinction based on the corresponding rates of initiation associated with each of those initiators, thereby leading to the prediction that for fast rates of initiation, the result will be a polymer film and for relatively slower rates of initiation, the fibrous polymer morphology will be obtained.

3.2. IR characterization of PECA samples

IR and Raman techniques have been used to study real time polymerization kinetics of alkyl cyanoacrylates [29–32]. These studies looked at characteristic differences in the spectral bands as monomer was consumed to make the polymer. In this study IR spectroscopy was used to examine differences in the chemical structure between the different PECA samples. The IR spectra of ECA monomer, vapor phase polymerized PECA-film and PECA-nanofiber samples and an ECA film that was cured under ambient conditions were compared. In this last sample the top layer of the liquid monomer is first initiated by moisture in the air which leads to subsequent propagation (curing) taking place in the liquid phase of the monomer until the entire film was completely polymerized. Fig. 5 depicts three regions of interest of the IR spectra obtained for the cured ECA film sample and the vapor phase polymerized film and nanofiber samples.

The ECA monomer IR spectrum was obtained by transmission-IR of a thin film of liquid monomer spread between two KBr pellets. The remaining three PECA samples were analyzed by ATR on polymer residue collected on a Si wafer. Peak assignments in the spectra were made by referring to characteristic IR absorption of the different functional groups [33]. Interestingly, the spectra for the two vapor phase polymerized PECA samples appear identical, suggesting that the chemical structure of the two morphologically different polymers is the same. However, some distinctions exist between these samples and the polymer made by curing the ECA film, which are discussed below.

In region I (Fig. 5(a), 3300–2700 cm^{-1}), the most prominent spectral change between the ECA monomer and PECA polymer is the disappearance of the peak at 3130 cm^{-1} in the polymer. The vibration at this frequency arises because of the $=CH_2$ stretching of the vinyl group present in the monomer, whereas for the PECA polymer chain this vinyl functionality does not exist and hence disappears. This is apparent in all the three polymer samples. Peaks between 3000 and 2800 cm^{-1} are due to the asymmetric and symmetric stretches of the $–CH_3$ and $–CH_2–$ groups. A noteworthy fact about the composition of the cured PECA-film is that it contains small amounts (up to 5%) of poly(methyl methacrylate) (PMMA). PMMA is present in the as received ECA monomer from Sirchie Fingerprint Lab Inc. to increase the viscosity of the adhesive for better application. The evidence of this PMMA is observed as an additional small peak at 2850 cm^{-1} because of symmetric C–H stretches of the $CH_3–O$ group. This peak is not detectable in the two vapor phase polymerized samples as they do not contain any PMMA.

In region II (Fig. 5(b), 2300–2200 cm^{-1}), the peak due to –CN stretching is seen at 2239 cm^{-1} in the ECA monomer. This peak is completely absent in the bulk liquid PECA-film and appears at higher wavenumbers and of a lesser intensity in the two vapor phase polymers. The shift of the –CN peak and reduction in its intensity has been observed previously in IR studies of alkylcyanoacrylate polymerization. The shift has been attributed to loss of conjugation between the –CN, C=C and C=O groups and because of the presence of –CN in two different environments [30], or because of the significant stablilization of the carbanion formed by delocalization of the negative charge, or an effect of inter- and intra-molecular hydrogen bonding [29]. However, at this point the cause of the decrease in intensity of the –CN peak is not known.

Region III (Fig. 5(c), 2000–1500 cm^{-1}) is important for two peaks, one at ~1730 cm^{-1} assigned for C=O stretching and one near 1615 cm^{-1} representing C=C stretching vibrations. The C=O peak shifts to a lower frequency for the bulk phase PECA-film and shifts to a slightly higher frequency for the vapor phase PECA. The net shift in position of the C=O peak usually is a result of a few factors that influence upward or downward shifts in the frequency

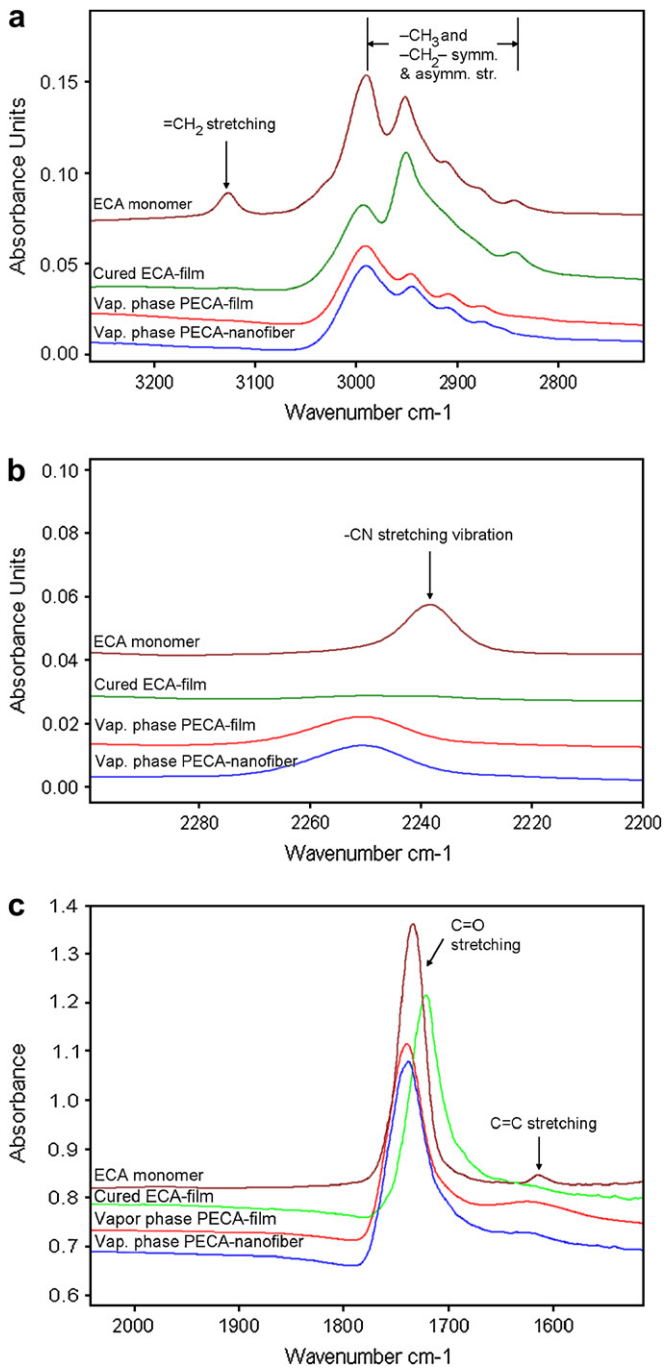

Fig. 5. IR spectra for different PECA samples showing (a) Region I: 3300–2700 cm^{-1}; (b) Region II: 2300–2200 cm^{-1} and (c) Region III: 2000–1500 cm^{-1}.

of IR absorption [33]. Some of the reasons causing such a decrease in frequency are, liquid monomer converting to solid polymer causing an increase in H-bonding interactions and resonance hybrids with the C=O group. The factor that causes an increase in the absorption frequency is the loss of unsaturation in the β-position because of polymer backbone formation. Hence it appears that for the vapor-grown PECA, the increase in frequency caused by polymer backbone formation is greater than the decrease in frequency caused by H-bonding or resonance hybrids. With regard to the C=C stretch, in going from the ECA monomer to the cured ECA film this peak disappears as expected with the elimination of the double bond in the monomer as the polymer backbone is formed. However, in the two vapor-grown PECA polymers a weak signal for this peak still exists. This can be explained by chain transfer steps occurring by hydride ion elimination (Scheme 2). Such chain transfer steps result in a dead polymer chain having a C=C at the end. These C=C ended chains account for the intensity of the peak at 1615 cm^{-1} to still be present in the polymer spectra. Hence this suggests that in the vapor phase polymerization significant chain transfer steps occur by H^- elimination.

To summarize, the IR investigation indicated no structural differences between the PECA-film and PECA-nanofiber sample that were deposited by vapor phase polymerization of the monomer. However, they did differ from a PECA polymer sample that was cured in the liquid phase. The differences suggesting that transfer steps in the vapor phase polymerization route occur via hydride ion elimination from the growing end of an active polymer chain.

3.3. Molecular weight estimations by GPC

Molecular weight estimations were obtained using a universal polystyrene calibration curve as the standard. The concentration of all the polymer samples injected in to the GPC was kept at approximately the same value of 1.5 mg/ml. The flowrate of solvent was maintained at 1 ml/min which gave a retention time of 40 min in the GPC columns. Fig. 6 presents the trace obtained from the refractive index (RI) detector on the GPC as a function of elution time for different polymer samples. The traces are for vapor phase polymerized PECA-nanofibers and PECA-film initiated by 1 M NaCl and 1 M NaOH, respectively.

Peak molecular weights are indicated for each major peak in all traces. Comparing the two vapor phase polymers, the PECA-film made by using NaOH as initiator has a higher molecular weight (15 123) than the PECA-nanofibers (6315) made using NaCl as the initiator. As the concentration of initiator used for making these two polymers was the same and the duration of polymerization was the same, the difference is due to the differences in the rates of initiation during their respective polymerizations. The IR analysis indicated that transfer or termination reactions are identical in these two PECA polymers implying that the lower molecular weight for PECA-nanofibers signifies a slower rate for initiation in contrast to the PECA-film polymerization. Correlating this observation with the classification of initiators already established there is an agreement with the observed trend in rates of initiation of polymerization and resulting molecular weights of the polymer. For *faster* rates of initiation with *harder* anions leading to PECA-film formation, the molecular weight of the polymer obtained is higher than that obtained by *slower* rates of initiation with *softer* anions leading to PECA-fiber formation.

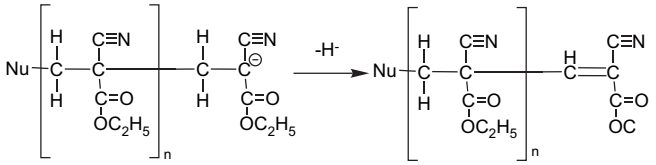

Scheme 2. Probable chain transfer route during vapor phase ECA polymerization.

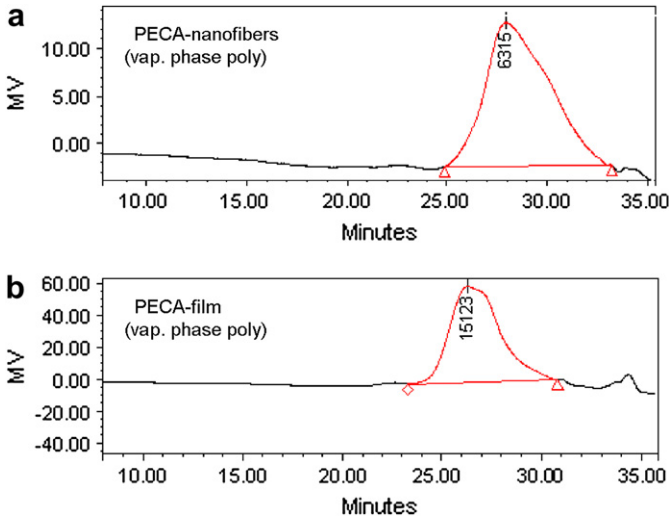

Fig. 6. GPC traces of (a) PECA nanofibers made via vapor phase polymerization using 1 M NaCl; (b) PECA film made via vapor phase polymerization using 1 M NaOH.

3.4. Mechanism of formation of different polymer morphologies during vapor phase polymerization

The IR investigation of the different PECA samples revealed that the two vapor phase PECA samples; film and nanofibers, were identical with respect to their chemical structure, hence the explanation of the different morphologies during polymerization must lie in the mechanism of polymer growth. The classification of the different initiators based on the HSAB principle and the molecular weight estimations by GPC that revealed higher molecular weight fractions in the PECA-film and lower molecular weight fractions in the PECA-fiber sample, confirmed that faster rates of initiation favored film formation (2-D growth) and relatively slower rates favored fiber formation (1-D growth). Based on these observations a suggested mechanism for formation of different polymer morphologies is put forth below.

The rates of initiation and propagation for polymerization can be written as

$$\mathrm{I}^- + \mathrm{M} \rightarrow \mathrm{P}^- \quad \text{Initiation}, \quad R_\mathrm{i} = k_\mathrm{i}\left[\mathrm{I}^-\right][\mathrm{M}]$$

$$\mathrm{P}_n^- + \mathrm{M} \rightarrow \mathrm{P}_{n+1}^- \quad \text{Propagation}: \quad R_\mathrm{P} = k_\mathrm{P}[\mathrm{M}]\left[\mathrm{P}_n^-\right]$$

where, I^-, M, P_n^-, n, Rs and ks are anionic initiator, monomer, active polymer chain, number of monomer units in a polymer chain, rates and rate constants, respectively. Since the concentrations of the initiator $[\mathrm{I}^-]$ and monomer [M] were kept constant between the different PECA samples, then $(k_\mathrm{i})_\mathrm{fiber} < (k_\mathrm{i})_\mathrm{film}$ or $(R_\mathrm{i})_\mathrm{fiber} < (R_\mathrm{i})_\mathrm{film}$. Therefore, at any instant after initiation, the concentration of growing polymer chains $[P_n^-]$ will always be lower in the PECA-nanofiber sample than the PECA-film sample. This initial inequality in concentration of active chains caused by the difference in rates of initiation results in fewer centers of growing polymer per unit area (localized sites of initiation) for the PECA-fiber as compared to the PECA-film polymer. As propagation continues, the fewer number of polymer chains growing per unit area have a growth front propagating in one direction, thus 'templating' the formation of 1-D nanofibers whereas relatively larger number of polymer chains growing per unit area have growth fronts in more than one direction, thereby 'templating' formation of a 2-D film. Hence the initial 'templating' effect that determines the ultimate polymer morphology is a function only of the rate constant for initiation, k_i. Chain transfer reactions affect both types of the growing polymers in the same manner. But because of the difference in the concentrations of active chains between the two polymers i.e. $[P_n^-]_\mathrm{fiber} < [P_n^-]_\mathrm{film}$, the overall progress of polymerization are also different, thereby causing the polymer nanofibers to have a lower average molecular weight than the polymer film.

4. Conclusions

In summary, we set out to answer some of the major questions regarding the mechanism of template-less formation of PECA-nanofibers during vapor phase polymerization of ethyl 2-cyanoacrylate. To explain the mechanism the influence of different types of anionic initiators for polymerization that resulted in polymer nanofibers or a textured polymer film was investigated. Anionic initiators were compared on the basis of their hygroscopicity and softness–hardness character. A suitable method for classifying the initiators studied was established by comparing their relative soft–hard character ($\mathrm{p}K_\mathrm{s} - \mathrm{p}K_\mathrm{a}$). There appeared to be a correlation between $\mathrm{p}K_\mathrm{s} - \mathrm{p}K_\mathrm{a}$ of the initiators and the observed morphology. Typically, a harder anion with a more rapid interaction with the hard acid center of the monomer would result in PECA-film formation whereas a softer anion with a slower interaction with the hard acid center of the monomer would result in PECA-nanofiber formation. This trend was also evident in the molecular weight analysis where the PECA-film showed a higher molecular weight than the PECA-nanofibers. IR spectra showed that there were no differences between the two vapor phase polymers with respect to their chemical structures, however, it did provide insight into the possible chain transfer steps that occur during vapor phase polymerization suggesting that transfer by hydride ion elimination is prominent. Finally, an explanation is proposed for the mechanism of formation of PECA-nanofiber and PECA-film which suggests that, the initial discrepancies between the rates of initiation causes localized sites of initiation in the case of slow rates that promotes 1-D fiber growth versus 2-D film morphology of the polymer when there is a greater concentration of initiation sites caused by faster rate of initiation.

Acknowledgements

This research was supported by National Science Foundation NIRT contract number DMI02-10229. The authors also wish to thank Josh Stapleton of The Pennsylvania State University's

Materials Characterization Laboratory for his assistance with the IR work in this study.

References

[1] Subbiah T, Bhat GS, Tock RW, Parameswaran S, Ramkumar SS. Journal of Applied Polymer Science 2005;96:557–69.
[2] Li D, Xia YN. Advanced Materials 2004;16(14):1151–70.
[3] Kim JS, Reneker DH. Polymer Composites 1999;20(1):124–31.
[4] Li WJ, Laurencin CT, Caterson EJ, Tuan RS, Ko FK. Journal of Biomedical Materials Research 2002;60(4):613–21.
[5] Kenawy ER, Bowlin GL, Mansfield K, Layman J, Simpson DG, Sanders EH, et al. Journal of Controlled Release 2002;81(1–2):57–64.
[6] Gibson P, Schreuder-Gibson H, Rivin D. Colloids and Surfaces A: Physicochemical and Engineering Aspects 2001;187:469–81.
[7] Martin CR. Science 1994;266(5193):1961–6.
[8] Li HY, Ke YC, Hu YL. Journal of Applied Polymer Science 2006;99(3):1018–23.
[9] Kageyama K, Tamazawa J, Aida T. Science 1999;285(5436):2113–5.
[10] Yu YJ, Si ZH, Chen SJ, Bian CQ, Chen W, Xue G. Langmuir 2006;22(8):3899–905.
[11] Huang JX, Kaner RB. Chemical Communications 2006;(4):367–76.
[12] Chien JCW, Yamashita Y, Hirsch JA, Fan JL, Schen MA, Karasz FE. Nature 1982;299(5884):608–11.
[13] Mankidy PJ, Ramakrishnan RB, Foley HC. Chemical Communications 2006;(10):1139–41.
[14] Skeist I. Handbook of adhesives. 3rd ed. New York: Van Nostrand Reinhold; 1990.
[15] Doiphode SV, Reneker DH, Chase GG. Polymer 2006;47(12):4328–32.
[16] Wagner RS, Ellis WC. Applied Physics Letters 1964;4(5):89–91.
[17] Levitt AP. Whisker technology. New York: Wiley-Interscience; 1970.
[18] Pearson RG. Journal of the American Chemical Society 1963;85(22):3533–9.
[19] Pearson RG. Science 1966;151(3707):172–7.
[20] Schwarze G, Schellen M. Helvetica Chimica Acta 1965;48(1):28–46.
[21] Alderighi L, Gans P, Midollini S, Vacca A. Inorganica Chimica Acta 2003;356:8–18.
[22] Sanz J, Raposo JC, de Diego A, Madariaga JM. Applied Organometallic Chemistry 2002;16(7):339–46.
[23] De Robertis A, Foti C, Patane G, Sammartano S. Journal of Chemical and Engineering Data 1998;43(6):957–60.
[24] Lide DR. CRC handbook of chemistry and physics special students edition. Boston: CRC Press; 1991.
[25] Pearson RG, Songstad J. Journal of the American Chemical Society 1967;89(8):1827–36.
[26] Pearson RG. Journal of Organic Chemistry 1989;54(6):1423–30.
[27] Huheey JE. Inorganic chemistry; principles of structure and reactivity. New York: Harper and Row; 1972.
[28] Donnelly EF, Johnston DS, Pepper DC, Dunn DJ. Journal of Polymer Science Part C: Polymer Letters 1977;15(7):399–405.
[29] Tomlinson SK, Ghita OR, Hooper RM, Evans KE. Vibrational Spectroscopy 2006;40(1):133–41.
[30] Edwards HGM, Day JS. Journal of Raman Spectroscopy 2004;35(7):555–60.
[31] Urlaub E, Popp J, Roman VE, Kiefer W, Lankers M, Rossling G. Chemical Physics Letters 1998;298(1–3):177–82.
[32] Yang DB. Journal of Polymer Science, Part A: Polymer Chemistry 1993;31(1):199–208.
[33] Socrates G. Infrared and Raman characteristic group frequencies: tables and charts. 3rd ed. Chichester, New York: Wiley; 2001.